

Microsimulation Model Calibration using Incremental Mixture Approximate Bayesian Computation

Carolyn Rutter¹, Jonathan Ozik², Maria DeYoreo¹, and Nicholson Collier²

¹RAND Corporation

²University of Chicago and Argonne National Laboratory

March 27, 2022

Abstract

Microsimulation models (MSMs) are used to predict population-level effects of health care policies by simulating individual-level outcomes. Simulated outcomes are governed by unknown parameters that are chosen so that the model accurately predicts specific targets, a process referred to as model calibration. Calibration targets can come from randomized controlled trials, observational studies, and expert opinion, and are typically summary statistics. A well calibrated model can reproduce a wide range of targets. MSM calibration generally involves searching a high dimensional parameter space and predicting many targets through model simulation. This requires efficient methods for exploring the parameter space and sufficient computational resources. We develop Incremental Mixture Approximate Bayesian Computation (IMABC) as a method for MSM calibration and implement it via a high-performance computing workflow, which provides the necessary computational scale. IMABC begins with a rejection-based approximate Bayesian computation (ABC) step, drawing a sample of parameters from the prior distribution and simulating calibration targets. Next, the sample is iteratively updated by drawing additional points from a mixture of multivariate normal distributions, centered at the points that yield simulated targets that are near observed targets. Posterior estimates are obtained by weighting sampled parameter vectors to account for the adaptive sampling scheme. We demonstrate IMABC by calibrating a MSM for the natural history of colorectal cancer to obtain simulated draws from the joint posterior distribution of model parameters.

1 Introduction

Microsimulation models (MSMs) are useful tools for predicting population-level effects of medical interventions on health outcomes because they synthesize information from randomized controlled trials, observational studies, and expert opinion. MSMs are characterized by simulation of *agents* that represent individual members of an idealized population of interest. For each agent, the model simulates event histories that catalog landmarks in the disease process, such as the development of an incident cancer. In general, the mechanisms driving these processes are not directly observable,

though outcomes from these processes can be observed. Model calibration involves selecting parameter values that result in model predictions that are consistent with observed data and expected findings. Once parameters are selected, MSMs can be used to make predictions about population trends in disease outcome, population-level effectiveness of interventions, and for estimating the comparative effectiveness of interventions that cannot otherwise be directly compared. For example, models have been used to inform U.S. Preventive Services Task Force screening guidelines for breast (Mandelblatt et al., 2016), cervical (Kim et al., 2017), colorectal (Knudsen et al., 2016), and lung cancer (de Koning et al., 2014).

MSM calibration involves searching a high dimensional parameter space to predict many targets; Several approaches have been proposed. The simplest calibration method involves perturbing parameters one at a time and evaluating the goodness of fit to calibration data, but this is only feasible when calibrating a few parameters. Directed searches, such as the Nelder-Mead algorithm (Nelder and Mead, 1965), provide a derivative free hill-climb to identify a single best value for each parameter. Kong et al. (2009) used automated parameter search algorithms from engineering (simulated annealing and a genetic algorithm) to find the optimal parameter set that yields the best fit.

Bayesian calibration methods estimate joint posterior distributions of model parameters. Estimated posterior distributions are useful because they provide information about parameter uncertainty. Markov Chain Monte Carlo (MCMC) algorithms are a standard tool for simulating draws from a posterior distribution of model parameters conditional on observed data. However, MCMC can be difficult and costly to apply to MSM calibration (Rutter et al., 2009) and because MCMC is based on a process of sequentially updating draws, it is not easy to parallelize the process to take advantage of modern computing resources.

Approximate Bayesian Computation (ABC) offers an alternative approach to MSM calibration. ABC is a suite of techniques used to simulate draws from the posterior distribution of model parameters given calibration targets that avoids estimation of the likelihood (Marin et al., 2012). However, ABC is inefficient and can fail when the parameter space is high dimensional, when there are many calibration targets, or when the prior distributions are very different from the posterior distributions. McKinley et al. (2017) found that popular ABC variants did not provide a computationally feasible approach for calibrating stochastic epidemiological models.

We propose an Incremental Mixture ABC (IMABC) for MSM model calibration. IMABC begins with a basic rejection-sampling ABC step (e.g., Pritchard et al., 1999) and then incrementally updates samples by adding points to regions of model fit. In the next sections we describe the CRC-SPIN MSM for the natural history of colorectal cancer (CRC) (§2), calibration targets used to inform CRC-SPIN model parameters (§3), the IMABC calibration approach (§4), and results of CRC-SPIN model calibration based on IMABC (§5). We conclude with general remarks about the proposed approach and discussion of future work (§6).

2 Microsimulation Model for the Natural History of Colorectal Cancer

The ColoRectal Cancer Simulated Population Incidence and Natural history model (CRC-SPIN) (Rutter et al., 2009; Rutter and Savarino, 2010) describes the natural history of CRC based on the adenoma-carcinoma sequence (Muto et al., 1975; Leslie et al., 2002). Four model components describe the natural history of CRC: 1) adenoma risk; 2) adenoma growth; 3) transition from adenoma to preclinical cancer; and 4) transition from preclinical to clinical cancer (sojourn time).

Model validation revealed that while CRC-SPIN predicted many aspects of disease well, it predicted too few preclinical cancers, indicating that simulated sojourn times were too short (Rutter et al., 2016). In this paper we present CRC-SPIN 2.0, a revised version of the original CRC-SPIN 1.0 model with an updated sojourn time model. Table 1 summarizes CRC-SPIN 2.0, which contains a total of 21 calibrated parameters. Because this is a model recalibration, prior distributions are based on results from the previous calibration of CRC-SPIN 1.0 (Rutter et al., 2009).

2.1 Adenoma Risk Model

The occurrence of adenomas is modeled using a non-homogeneous Poisson process with a piecewise age-effect. The i th agent’s instantaneous risk of an adenoma at time t is given by

$$\psi_i(t) = \exp \left(\alpha_{0i} + \alpha_1 sex_i + \sum_{k=1}^4 \delta_k(age_i(t)) \left\{ age_i(t) \alpha_{2k} + \sum_{j=2}^k a_j (\alpha_{2j-1} - \alpha_{2j}) \right\} \right) \quad (1)$$

where $\alpha_{0i} \sim N(A, \sigma_\alpha)$ describes an agent’s baseline risk, α_1 describes the difference in risk for men ($sex_i = -1$) versus women ($sex_i = +1$), α_{2k} describes changes in risk with age (in years) in the k th interval, and $\delta_k(age_i(t)) = 1$ when $a_k < age_i(t) \leq a_{k+1}$ and is zero otherwise. The change-point model for adenoma risk specifies that agents are not at risk of developing adenomas until age $a_1 = 20$ and that risk changes at ages $a_2 = 50$, $a_3 = 60$, and $a_4 = 70$, with a maximum age of $a_5 = 120$. This is the same adenoma risk model used in CRC-SPIN 1.0, with the exception that age-effects can be negative after age 60 years to allow declining risk of adenoma initiation.

Once adenomas are initiated they are assigned a location. The distribution of adenomas throughout the large intestine follows a multinomial distribution based on data from 9 autopsy studies (Blatt, 1961; Chapman, 1963; Stemmermann and Yatani, 1973; Eide and Stalsberg, 1978; Rickert et al., 1979; Williams et al., 1982; Bombi, 1988; Johannsen et al., 1989; Szczepanski et al., 1992). The probabilities associated with six sites in the large intestine (from distal to proximal) are: P(rectum) = 0.09; P(sigmoid colon) = 0.24; P(descending colon) = 0.12; P(transverse colon) = 0.24; P(ascending colon) = 0.23; and P(cecum) = 0.08. For many purposes it is important to distinguish between colon and rectal locations; more detailed location information is sometimes used for determining screening test accuracy.

Table 1: Summary of CRC Microsimulation Model Components. Calibrated parameters associated with the 4 components of the natural history model, including parameter notation, associated equations, prior distributions and posterior estimates (mean and 95% credible interval). $TN_{[a,b]}(\mu,\sigma)$ denotes a truncated normal distribution with mean μ and standard deviation σ , restricted to the interval (a,b) . $U(a,b)$ denotes a Uniform distribution over (a,b) . Refer to section 2 for details of the 4 model components.

Component	Prior Distribution	Posterior Estimates	
		Mean	95% CI
Adenoma Risk (eqn 1)			
Baseline log-risk	$A \sim TN_{[-7.6,-5.6]}(-6.6,1.0)$	-6.86	(-7.17,-6.54)
Main sex effect	$\alpha_1 \sim TN_{[-0.55,-0.05]}(-0.24,0.1)$	-0.34	(-0.42,-0.27)
Standard Deviation, baseline log-risk	$\sigma_\alpha \sim U(0.5,2.0)$	1.31	(1.05,1.68)
Age effect, age $\in [20, 50)$	$\alpha_{20} \sim TN_{[0.01,0.06]}(0.037,0.06)$	0.052	(0.042,0.059)
Age effect, age $\in [50, 60)$	$\alpha_{21} \sim TN_{[0,0.06]}(0.031,0.01)$	0.023	(0.016,0.030)
Age effect, age $\in [60, 70)$	$\alpha_{22} \sim TN_{[-0.04,0.05]}(0.029,0.01)$	0.031	(0.021,0.039)
Age effect, age ≥ 70	$\alpha_{23} \sim TN_{[-0.04,0.05]}(0.030,0.12)$	-0.001	(-0.036,0.042)
Time to 10mm (eqn 2)			
colon	$\beta_{\text{colon}} \sim U(12,30)$	27.6	(25.2,28.9)
rectum	$\beta_{\text{rectum}} \sim U(12,30)$	14.1	(12.9,15.2)
colon	$\alpha_{\text{colon}} \sim U(1.1,3)$	1.30	(1.11,1.53)
rectum	$\alpha_{\text{rectum}} \sim U(1.1,3)$	1.84	(1.25,2.27)
Transition to Cancer (eqn 3)			
Intercept	$\gamma_0 \sim TN_{[2.6,3.6]}(3.1,0.5)$	3.39	(3.31, 3.47)
Female	$\gamma_1 \sim TN_{[-0.5,0.3]}(-0.06,0.2)$	-0.15	(-0.24, -0.07)
Rectal location	$\gamma_2 \sim TN_{[-0.05,0.5]}(0.25,0.25)$	-0.16	(-0.29, -0.02)
Female & rectal location	$\gamma_3 \sim TN_{[-0.35,0.25]}(-0.14,0.20)$	0.07	(-0.07, 0.18)
Age at initiation	$\gamma_4 \sim TN_{[-0.012,0.004]}(-0.008,0.016)$	-0.007	(-0.013,-0.001)
Female & age at initiation	$\gamma_5 \sim TN_{[-0.007,0.013]}(0.003,0.012)$	0.002	(-0.004, 0.008)
Rectal & age at initiation	$\gamma_6 \sim TN_{[-0.002,0.020]}(-0.016,0.008)$	-0.004	(-0.011,0.002)
Female, rectal, & age at initiation	$\gamma_7 \sim TN_{[-0.024,-0.016]}(-0.008,0.020)$	-0.001	(-0.011, 0.008)
Mean Sojourn Time (eqn 4)			
Colon	$\tau_{\text{colon}} \sim U(1.5,7.0)$	3.05	(2.19,4.06)
Rectum	$\tau_{\text{rectum}} \sim U(1.5,7.0)$	3.28	(2.68,3.78)

2.2 Adenoma Growth Model

Adenoma growth is modeled using an extension to the Janoschek growth curve model (Janoschek, 1957; Gille and Salomon, 2000). For the j th adenoma in the i th agent at time t after onset, the diameter of the adenoma is equal to $d_{ij}(t) = d_\infty - (d_\infty - d_0)e^{-\lambda_{ij}t}$, where $d_\infty = 50$ is the maximum adenoma diameter in millimeters (mm), $d_0 = 1$ mm is the minimum adenoma diameter, and λ_{ij} is the growth rate for the j th adenoma within the i th agent. This model is asymmetric, with exponential growth early that slows to allow an asymptote at d_∞ .

To improve our ability to relate adenoma growth to observable data and clinical knowledge, we parameterize the growth model in terms of the time it takes for the adenoma diameter to reach 10mm, $t_{10mm} = -\frac{1}{\lambda} \ln\left(\frac{d_\infty - 10}{d_\infty - d_0}\right)$. We assumed that t_{10mm} has a Fréchet (or type II extreme value) distribution with shape parameter α , scale parameter β , and cumulative distribution function given by

$$F(t) = \exp\left[-\left(\frac{t}{\beta}\right)^{-\alpha}\right] \quad (2)$$

for $t \geq 0$. The Fréchet distribution has a long right tail, with skewness that can persist as the mean moves away from zero, allowing for a large proportion of slow growing adenomas. Under this model, $E(t_{10}) = \beta\Gamma(1 - 1/\alpha)$, with median $\beta/\ln(2)^{1/\alpha}$. Prior distributions for adenoma growth parameters specify that most adenomas grow very slowly, with at most 29% of adenomas reaching 10mm within 10 years, and potentially far fewer growing this quickly. This is the same model used in CRC-SPIN 1.0. We allow the scale and shape parameters to be location-specific.

2.3 Model for Transition from Adenoma to Preclinical Invasive Cancer

The CRC-SPIN 2.0 uses a reparameterized version of the CRC-SPIN 1.0 model for adenoma transition, restated as a regression model to better evaluate differences based on agent and adenoma characteristics. The size at transition to preclinical cancer (in mm) for each adenoma is simulated using a lognormal distribution. The underlying (exponentiated) normal distribution has standard deviation 0.5 and mean

$$\begin{aligned} \mu_\gamma = & \gamma_0 + \gamma_1\delta_f + \gamma_2\delta_r + \gamma_3\delta_f\delta_r + \\ & \left(\gamma_4 + \gamma_5\delta_f + \gamma_6\delta_r + \gamma_7\delta_f\delta_r\right)(\text{age at initiation} - 50). \end{aligned} \quad (3)$$

Where $\delta_f = 1$ if the agent is female and is zero otherwise and $\delta_r = 1$ if the adenoma is located in the rectum and is zero otherwise. Based on this model, the expected size at transition is given by $\exp(\mu_\gamma + 0.125)$, with median $\exp(\mu_\gamma)$ and variance $0.28 \exp(2\mu_\gamma + 0.25)$. Negative parameter values indicate that transition tends to occur at smaller adenoma sizes. Under this model, most adenomas do not reach transition size and small adenomas are unlikely to transition to cancer. For example, if $\mu_\gamma = 3.5$ then the probability of transition to preclinical cancer is less than 0.00001 at 10mm, 0.008 at 15mm and 0.16 at 20mm.

2.4 Model for Sojourn Time

Sojourn time is modeled using a Weibull distribution with shape parameter fixed at 5, given by:

$$f(x) = \left(\frac{5}{\tau}\right) \left(\frac{x}{\tau}\right)^4 \exp\left(-\left(\frac{x}{\tau}\right)^5\right) \quad (4)$$

with $E(x) = \tau\Gamma(1.2)$ and $Var(x) = \tau^2(\Gamma(1.4) - \Gamma(1.2)^2)$. By fixing the shape parameter, we focus on distributions with a limited range of skewness, disallowing distributions with heavy right tails while allowing sufficient flexibility to model plausible sojourn time distributions. Sojourn time is assumed to be independent across preclinical cancers within agents, and depends on location (colon or rectum). Prior distributions for sojourn time parameters allow mean sojourn time to range from 1.4 (with SD 0.32) to 6.4 years (SD equal to 1.5).

2.5 Simulation of Lifespan and Colorectal Cancer Survival

Once a cancer becomes clinically detectable, we simulate stage and size at clinical detection and survival. Stage and tumor size at clinical detection are based on SEER data from 1975 to 1979, prior to diffusion of CRC screening (National Cancer Institute, 2004). Simulated survival time after CRC diagnosis is based on a Cox proportional hazards model, estimated using SEER data from individuals diagnosed with CRC from 1975 through 2003 (Rutter et al., 2013). CRC survival is based on the first diagnosed CRC and depends on sex, age at diagnosis, cancer location (colon or rectum) and stage at diagnosis.

Other-cause mortality is modeled using survival probabilities based on product-limit estimates for age and birth-year cohorts from the National Center for Health Statistics Databases (National Center for Health Statistics, 2000).

3 Calibration Data

Calibration data are derived from published studies, and typically take the form of summary statistics with known distributions, such as binomial, multinomial, and Poisson. We calibrate to 37 targets from six sources: SEER registry data (16 targets) (National Cancer Institute, 2004), four epidemiologic studies (19 targets), and a case series (two targets). We also incorporated information about adenoma growth from a recent study that examined individuals with two screening colonoscopies that were approximately ten years apart (Ponugoti and Rex, 2017). The second screening colonoscopy detected advanced adenomas (defined as adenomas ≥ 10 mm in size, or with villous features or high-grade dysplasia) in 3% of individuals overall and in 9% of individuals with at least one adenoma. Based on this, we bounded adenoma growth parameters so that the percent of adenomas reaching 10mm within 10 years ranged from 1% to 25%.

Below we describe each of the calibration sources and information used to simulate corresponding calibration targets.

Table 2: Annual Incidence of Clinically Detected Cancers in 1975-1979, per 100,000 individuals.

		SEER Population	Rectal Cancer	Colon Cancer
Female	20-49	4,388,669	1.9	4.8
Female	50-59	1,130,418	20.4	43.3
Female	60-69	851,298	42.5	100.7
Female	70-84	835,820	73.9	216.7
Male	20-49	4,322,108	2.3	4.5
Male	50-59	1,055,100	30.0	45.9
Male	60-69	734,756	71.4	121.4
Male	70-84	519,982	128.0	268.4

3.1 Aggregated Individual-level data

Calibration to individual-level data requires simulating a set of agents with risk that is similar to the study population based on age, gender, and prior screening patterns. Simulations also account for the time period of the study, which affects both overall and cancer-specific mortality. In general, studies describe their samples by reporting the percentage of men and women, their average age, and the standard deviation of age. Unless information was provided by sex, we assumed the same age distribution for men and women. We modeled age distributions used in simulations using truncated normal distributions based on the reported means, standard deviations, and age ranges.

3.1.1 SEER Data

SEER colon and rectal cancer incidence rates in 1975-1979 are a key calibration target (Table 2). Incidence rates reported are per 100,000 individuals. These rates are based on the first observed invasive colon or rectal cancer during the years 1975-1979, the most recent period prior to dissemination of CRC screening tests. We assume that given the SEER population size, the number of cancer cases in any year follows a binomial distribution.

To simulate SEER incidence rates, we generate a population of individuals from 20 to 100, with an age- and sex-distribution that matches the SEER 1978 population who are free from clinically detected CRC. Model-predicted CRC incidence is based on the number of people who develop CRC in the next year.

3.1.2 Data from Epidemiologic Studies

Table 3 summarizes calibration targets from epidemiologic studies. To simulate these targets, we generated separate populations for each target that match the age and gender distribution of study participants.

Because participants in the Pickhardt et al. (2003) study underwent both colonoscopy and CT colonography, with a focus on comparing the sensitivity of these two modalities, we assume that in this study all adenomas were detected (i.e., perfect sensitivity). Studies by Corley et al. (2013), Im-

periale et al. (2000), and Lieberman et al. (2000) report findings from colonoscopy. Our simulations assume no screening prior to this exam, and that study participants are free from symptomatic (clinically detectable) CRC at the time of colonoscopy. When simulating model predictions for these studies the model incorporates colonoscopy sensitivity. We assumed a quadratic model for colonoscopy sensitivity based on lesion (i.e., adenoma or preclinical cancer) size (s). For adenomas, we assume $P(\text{miss}|\text{size} = s < 20\text{mm}) = 0.34 - 0.0349s + 0.0009s^2$ and $P(\text{miss}|\text{size} = s \geq 20\text{mm}) = 0$. This function results in sensitivity that is consistent with observed findings from the 1990's (Hixson et al., 1990; Rex et al., 1997): sensitivity is 0.76 for a 3mm adenoma, 0.87 for a 7.5mm adenoma, and 0.95 for a 12mm adenoma. For preclinical cancers, we assume sensitivity that is the maximum of 0.95 and sensitivity based on adenoma size, so that colonoscopy sensitivity is 0.95 for preclinical cancers 12mm or smaller, and sensitivity is greater than 0.95 for preclinical cancers larger than 12mm.

3.1.3 Adenoma Data

Data from a case series (Church, 2004), describes the pathology of 2,980 lesions (i.e., adenomas and preclinical cancers) removed between January 1995 and September 2002 in a single endoscopist's practice. For the purpose of calibration, we focus on preclinical cancer rates in lesions $\geq 6\text{mm}$ because very few cancers were detected in lesions $< 6\text{mm}$ (2 in 2066). Among 418 lesions 6 to 10mm, 1 cancer was detected (0.24%) and among lesions 10mm or larger 21 adenomas were detected (4.2%). Because this study did not provide information about the age or sex of patients, we calibrate to these targets by simulating a population that was 50% male with an average age of 65 with a standard deviation of 5, and an age range of 20 to 90 years. We assume that all adenomas are detected via colonoscopy, which may impact the size distribution.

4 Posterior Inference via Incremental Mixture Approximate Bayesian Computation (IMABC)

Approximate Bayesian computation methods are likelihood-free techniques for simulating draws from the posterior distribution of model parameters given data. The general idea is to replace the calculation of a likelihood with an approximation based on matching model simulations to the observed data using a set of goodness-of-fit metrics (Conlan et al., 2012). Using the basic rejection-based ABC algorithm (Tavare et al., 1997; Pritchard et al., 1999), the model parameter vector θ is generated from the prior distribution $\pi(\theta)$ and the model is used to simulate data, y^* . Draws that result in simulated data that are similar to observed data, y , are accepted. Similarity between y^* and y is based on user-defined summary statistics, $f(y)$, a distance metric, ρ , and a tolerance level, ϵ .

In practice, simulating θ from the prior distribution can be very inefficient, because the prior and posterior distributions are often poorly aligned. Many versions of ABC have been developed

Table 3: Calibration Data from Epidemiologic Studies Reporting Individual-Level Outcomes. Age is in years.

Prevalence of adenomas and preclinical cancers (Corley et al., 2013)		
Date range: 1/1/2006 - 12/31/2008		
Age Range	Sample Size	Adenoma Prevalence
Women		
50-54	3195	0.15
55-59	2599	0.18
60-64	2718	0.22
65-69	1665	0.24
70-74	1052	0.26
≥75	777	0.26
Men		
50-54	2398	0.25
55-59	1894	0.29
60-64	1873	0.31
65-69	1238	0.34
70-74	755	0.39
≥75	628	0.31
Overall number and size distribution of adenomas (Pickhardt et al., 2003)		
Date range: 1/1/2002 - 6/30/2003		
Mean age: 57.8		
Percent male: 59%		
Total sample size: 1233		
Age Range	Adenoma Size	Adenomas N=544
40-79	< 6mm:	0.620
	[6, 10)mm:	0.287
	≥ 10mm:	0.092
Number of Preclinical Cancers Detected, (Imperiale et al., 2000)		
Date range: 9/1/1995 - 12/31/1998		
Mean(SD) age: 59.8 (8.3)		
Percent male: 59%		
Age Range	Sample Size	Prevalence
≥ 50	1994	0.0035 (n=7)
Polyp size and preclinical cancer prevalence (Lieberman et al., 2008)		
Date range: 1/1/2005-12/31/2005		
Age distribution: [20,50): 7.6%; [50,60):48.4%; [60,70): 27.7%; [70,80):13.5%; [80,90):2.8%		
Percent male: 53%		
Age Range	Adenoma Size	Cancer Prevalence
≥ 20	[1, 6)mm	1 in 1880*
	[6, 10)mm	2 in 811
	≥ 10mm	25 in 778

*Data point not used as a calibration target

to address inefficiencies. Two popular variants are ABC-MCMC (Marjoram et al., 2003) and sequential Monte Carlo ABC (ABC-SMC) (Sisson et al., 2007; Toni et al., 2009).

ABC-MCMC involves proposing a new value of θ by sampling from a Markov kernel that is typically centered at the previous draw, $\theta^{(t-1)}$, $q(\theta | \theta^{(t-1)})$. If a new draw yields simulated data y^* that is not close to the observed data y ($\rho(f(y), f(y^*)) > \epsilon$), it is immediately rejected. Otherwise, the probability of acceptance depends on the ratio of $q(\theta | \theta^{(t-1)})\pi(\theta)$ to $q(\theta^{(t-1)} | \theta)\pi(\theta^{(t-1)})$. Drawbacks of ABC-MCMC include the usual problems with MCMC, such as correlated samples, low acceptance rates, the possibility of getting stuck in low posterior probability regions, and slow mixing requiring very long chains.

ABC-SMC is a parallel sequential ABC algorithm. The algorithm begins by simulating an initial set of draws. At each subsequent iteration, t , a new set of values $\theta_1^{(t)}, \dots, \theta_N^{(t)}$ is drawn by perturbing the previous set of draws $\theta_1^{(t-1)}, \dots, \theta_N^{(t-1)}$. Simulated draws from the posterior distribution are obtained by sampling θ 's that are within the tolerance region using weighted sample selection with importance weights based on the perturbation distribution. ABC-SMC allows the tolerance level to vary, becoming more stringent across iterations. As the tolerance level is reduced, the approximate posterior distribution should converge towards the true posterior distribution. The population Monte Carlo ABC algorithm (ABC-PMC) is closely related to ABC-SMC, drawing on ideas of importance sampling (Beaumont et al., 2009; Marin et al., 2012). At each iteration, ABC-PMC uses a kernel approximation to the target distribution based on previous iterations. New points are sampled via a component-wise independent random walk, a normal distribution centered at a previously accepted point chosen using importance weights. This effectively yields a normal mixture sampling distribution.

In general, ABC and its variants can be impractical or can fail when the parameter space is high dimensional (Blum and Francois, 2010), or there are many summary statistics that the simulated data must approximate. As discovered by McKinley et al. (2017), this precludes their use in the context of MSMs, where there are usually many calibration targets. To address the problems with ABC and MCMC in the context of MSMs, we propose a new ABC approach that we call incremental mixture approximate Bayesian computation (IMABC).

4.1 The IMABC algorithm

The IMABC algorithm begins with a rejection-sampling ABC step, and updates draws by adding points near draws that are nearest to targets. Because calibration targets are summary statistics from published studies, we directly compare simulated targets to published targets. We base the ABC distance metric and tolerance levels on the $(1 - \alpha_j) \times 100\%$ confidence intervals of calibration targets, allowing tolerance levels to vary across targets. Let O_1, \dots, O_J indicate calibration targets and let S_{ij} be the j th simulated target (corresponding to O_j) for the i th sampled point. We use an intersection approach for our distance metric (Conlan et al. (2012), Ratmann et al. (2014)) and define $\delta(\theta_i, \alpha) = 1$ if all S_{ij} , $j = 1, \dots, J$ fall within the $(1 - \alpha_j) \times 100\%$ confidence intervals for the targets O_j . Larger values of α_j imply tighter confidence intervals, i.e., more stringent requirements

for acceptance of points. For a given value of α , tolerance limits will be wider for less precisely estimated targets.

At the first IMABC step, a sample of N_0 points, $\theta_1, \dots, \theta_{N_0}$, is drawn from the prior distribution of model parameters, $\pi(\theta)$. Latin hypercube sampling can be used to ensure coverage of the parameter space. After this first step, the IMABC algorithm begins an updating phase, adding points in the neighborhood of $N^{(c)}$ “best” points, those that result in simulated targets, S_{ij} , closest to the observed targets, O_j . At each iteration, the $\alpha_j^{(k)}$ may be increased until it reaches a prespecified level, α_j^* . Initial α -levels, $\alpha_j^{(0)}$, may be very small.

Let N_t be the number of samples of θ drawn up to and including iteration t . The t th iteration in the IMABC algorithm for $t > 0$ proceeds as outlined below:

1. For accepted θ_i , i.e., $\{\theta_i, i = 1, \dots, N_{t-1} : \delta(\theta_i, \alpha^{(t-1)}) = 1\}$:
 - (a) Calculate two-sided p-values, p_{ij} , corresponding to the test of $H_0: S_{ij} = O_j$ for $j = 1, \dots, J$.
 - (b) Calculate $p_i = \min_j(p_{ij})$, the minimum p-value across targets corresponding to the worst fit for the i th point across targets.
2. Select the $N^{(c)}$ points with the largest p_i , $\theta_{(k)}^{(t)}$, $k = 1, \dots, N^{(c)}$.
 - (a) Simulate B new draws around each of the $\theta_{(k)}^{(t)}$ by sampling from a normal distribution with mean $\theta_{(k)}^{(t)}$ and covariance $\Sigma_{(k)}^{(t)}$. $\Sigma_{(k)}^{(t)}$ is calculated using the $N^{(B)}$ accepted points nearest to $\theta_{(k)}^{(t)}$.
 - (b) Resimulate targets corresponding to center points $\theta_{(k)}^{(t)}$. This step is used to avoid getting stuck at center points with simulated targets that are, by chance, very close to observed targets.
3. If any $\alpha_j^{(t-1)} < \alpha_j^*$ and there are $N^{(\alpha)}$ or more accepted points, check to see if the tolerance can be updated. For the set of targets, with $\alpha_j^{(t-1)} < \alpha_j^*$:
 - (a) Identify i' associated with median p_{ij} . For each potentially updated tolerance level, set $\alpha_j^{(t)} = \min(\alpha_j^*, p_{i'j})$.
 - (b) Update the acceptable points based on $\alpha^{(t)}$.

Otherwise leave α unchanged, letting $\alpha_j^{(t)} = \alpha_j^{(t-1)}$.
4. If $\alpha^{(t)} = \alpha^*$, determine whether the stopping criteria based on the effective sample size (ESS) has been met.
 - (a) Calculate sampling weights that account for the difference between the prior and mixture sampling distributions, $w_i = \pi(\theta_i)/q_t(\theta_i)$. The mixture sampling distribution, q_t is given by $q_t = \frac{N_0}{N_t}\pi + \frac{B}{N_t} \sum_{s=1}^t \sum_{k=1}^{N^{(c)}} H_k^{(s)}$ where $H_k^{(s)}$ is the k th normal distribution at iteration

t , given by $N(\theta_{(k)}^{(t)}, \Sigma_{(k)}^{(t)})$, and $N_t = N_0 + N^{(c)}Bt$, the total number of draws through iteration t .

- (b) Calculate the effective sample size (ESS) for the N_t draws, $(\sum_{i=1}^{N_t} w_i^2)^{-1}$, where $w_i = 0$ if $\delta(\theta_i, \alpha^{(t)}) = 0$ (Kish, 1965; Liu, 2004).
- (c) If $\text{ESS} \geq N_{post}$, the desired number of draws from the posterior distribution, the algorithm is complete. Otherwise, continue to iterate, but without further updates to the tolerance level at step 3.

Once the IMABC algorithm is complete, independent draws from the posterior distribution are simulated by taking a weighted sample from accepted points with replacement, using the w_i . These weights account for sampling of points from the normal mixture rather than the prior distribution.

The IMABC algorithm includes several tuning parameters: N_0 , the initial number of draws from the prior distribution; $N^{(\alpha)}$, the number of points that must be accepted before possibly updating the tolerance level; $\alpha^{(0)}$, the initial tolerance level; α^* , the target tolerance level; $N^{(c)}$, the number of normal mixtures used to draw new points at each step; $N^{(B)}$ the number of draws used to calculate the covariance matrix for each normal mixture; B , the number of points drawn at each of the $N^{(c)}$ mixture distributions; and N_{post} the effective sample size of the final set of accepted points. We recommend using a large initial sample size N_0 when using noninformative priors, because most initial sampled points will not lie in high posterior probability regions.

5 CRC-SPIN 2.0 Calibration Results

5.1 IMABC Implementation

In our application, we set $N_0 = 10,000$; $N^{(\alpha)} = 100$; $N^{(c)} = 10$; $N^{(B)} = 980$; $B = 1,000$; and $N_{post} = 5,000$. Using $N^{(c)} = 10$ centers allowed us to take advantage of processor concurrency. In Step 1(b) we chose to summarize p_{ij} by $p_i = \min_j(p_{ij})$, i.e., by the worst fitting target, but other choices such as $p_i = \text{mean}_j(p_{ij})$ may also be reasonable. We set $\alpha^{(0)} = \alpha^* = 0.001$ for Corley et al. (2013), Imperiale et al. (2000), Church (2004), and Lieberman et al. (2008) targets. We use a wider tolerance for the Pickhardt et al. (2003) target, with $\alpha^{(0)} = \alpha^* = 0.0001$, because it was difficult to reconcile these targets with bounds specified for the fraction of adenomas reaching 10mm within 10 years. For SEER data we began with $\alpha^{(0)} = 1 \times 10^{-20}$ and worked toward $\alpha^* = 1 \times 10^{-9}$. While this is a small α level, it still results in narrow bands around registry-based incidence rates.

When simulating calibration targets, we assumed no prior screening. Colorectal cancer screening guidelines have been in place since the late 1990s (Winawer et al., 1997), and screening rates have since risen steadily (Meissner et al., 2006; Centers for Disease Control & Prevention, 2011). Most studies were conducted prior to widespread screening, making this a generally reasonable assumption. However, the Corley et al. (2013) study is based on insured patients who underwent colonoscopies from 1/1/2006 to 12/31/2008. While this sample was selected to be minimally screened, when calibrating to this target we allowed tolerance limits to be up to 50% higher than

expected, to acknowledge that adenoma prevalence in this study may be lower than expected in a completely unscreened population.

Using IMABC to calibrate an MSM requires multiple model evaluations at each parameter draw, and the user needs to specify the size of draws used to simulate S_{ij} . These embedded simulation sizes, m , need to be large enough to allow accurate estimation of calibration targets at each parameter value. Setting m too low will result in inaccurate identification of acceptable θ_j . Setting m too large will unnecessarily slow the algorithm. We used embedded simulation sizes of 5×10^4 for Pickhardt et al. (2003); 2×10^5 for Corley et al. (2013) and Imperiale et al. (2000); 3×10^5 for Church (2004), 5×10^5 for Lieberman et al. (2008) and 5×10^6 for the SEER registry data.

When implementing the IMABC algorithm we recommend sequentially evaluating the targets at step 1, beginning with targets that are less computationally intensive (with smaller m). Once any simulated target is out of bounds, the point is rejected and there is no need to simulate the remaining, more computationally intensive, targets.

5.1.1 Programming and Computing Environment

Both the IMABC algorithm and the CRC-SPIN 2.0 model were implemented in the R programming language. We utilized the Extreme-scale Model Exploration with Swift (EMEWS) framework (Ozik et al., 2016) to implement a dynamic HPC workflow controlled by the IMABC algorithm. EMEWS, built on the general-purpose parallel scripting language Swift/T (Wozniak et al., 2013), allows for the direct integration of multi-language software components, in this case IMABC and CRC-SPIN 2.0, and can be implemented on computing resources ranging from desktops and campus clusters to supercomputers. The resulting IMABC EMEWS workflow is driven directly by the IMABC R source code, obviating the need for porting the code to alternate programming languages or platforms for the sole purpose of running large-scale computational experiments.

The experiments were performed on the Cray XE6 Beagle at the University of Chicago, hosted at Argonne National Laboratory. Experiments were also run on the Midway2 cluster at the University of Chicago Research Computing Center.

The IMABC algorithm completed 14 iterations, obtaining 5,607 parameter draws within tolerance limits, with an effective sample size of 5,504 draws from the joint posterior distribution. Sampling weights ranged from 1.2×10^{-4} to 5.0×10^{-4} , with a mean of 1.8×10^{-4} and median of 1.7×10^{-4} . The experiment used 80 nodes on Beagle and 4 worker processes per node (to account for the memory footprint of CRC-SPIN 2.0) for a total of 320 worker processes, each of which could concurrently execute an individual model run. The total compute time was 29.4 hours or 2,352 node-hours.

5.2 Estimated Posterior Distributions

Posterior estimated means and 95% credible intervals (CIs) for mode parameters were based on weighted means and percentiles of accepted draws from the joint posterior distribution (shown

in Table 1). Alternatively, one can simulate independent draws from the posterior by taking a weighted sample with replacement from the set of accepted points.

Estimates indicate that adenoma risk is higher for men than women, and continues to rise to age 70, when risk stabilizes. However, estimated 95% CIs indicate that we have little information about how adenoma risk changes after age 70.

Parameters that govern the time for an adenoma to reach 10mm were tightly estimated, with adenomas in the rectum reaching 10 mm faster than those in the colon. Under this model, most adenomas do not reach 10mm. The posterior 95% CIs for the median time to reach 10mm is 36.6 years with 95% CI (33.7,39.7) for adenomas in the colon and 17.3 years with 95% CI (15.8,19.6) for adenomas in the rectum. The posterior estimates of the proportion of adenomas that reach 10mm within 10 years is 0.025 with 95% CI (0.011,0.044) for adenomas in the colon and 0.155 with 95% CI (0.081,0.216) for adenomas in the rectum.

Model calibration results indicate that adenomas transition to preclinical cancer at smaller sizes for women, for adenomas in the rectum, and for adenomas initiated at later ages. We did not find evidence of differential effects of age at adenoma initiation on size at transition by adenoma location or agent sex (based on interaction terms γ_5 , γ_6 , and γ_7).

Estimated mean sojourn time was similar for preclinical cancers in the colon and rectum. The posterior 95% CIs for mean sojourn time is 2.8 years with 95% CI (2.00,3.72) for preclinical cancers in the colon and 3.0 with 95% CI (2.46,3.47) for preclinical cancers in the rectum. A contour plot of the bivariate posterior distribution for MST in the colon and the rectum is displayed in Figure 1.

By simulating draws from the posterior distribution, we were able to examine correlations among model parameters. For example, Figure 1 displays the bivariate posterior distributions of baseline log-adenoma risk (A) and the annual increase in risk between the ages of 20 and 50 years (α_{20}); When baseline risk is lower, risk increases more rapidly from 20 to 50 years (correlation is -0.67). As the shape parameter increases, the scale parameter must decrease in order to have significant mass at small values, which is required to allow some faster growing adenomas (with shorter time to reach 10mm).

6 Discussion

In previous work, we proposed an MCMC algorithm to calibrate MSM model parameters (Rutter et al., 2009). While this method was successful in obtaining draws from the posterior distribution, it had a number of drawbacks stemming from poor mixing and high correlation between sequential iterations, as well as subjectivity in determining convergence. We developed an ABC algorithm that avoids these difficulties, built on the ideas of incremental mixture importance sampling (IMIS) (Steele et al., 2006; Raftery and Bao, 2010), an adaptive Sampling Importance Resampling algorithm (SIR; Rubin, 1987). Like IMIS, the IMABC algorithm iteratively updates the proposal distribution at each iteration to obtain samples from regions of the parameter space that are con-

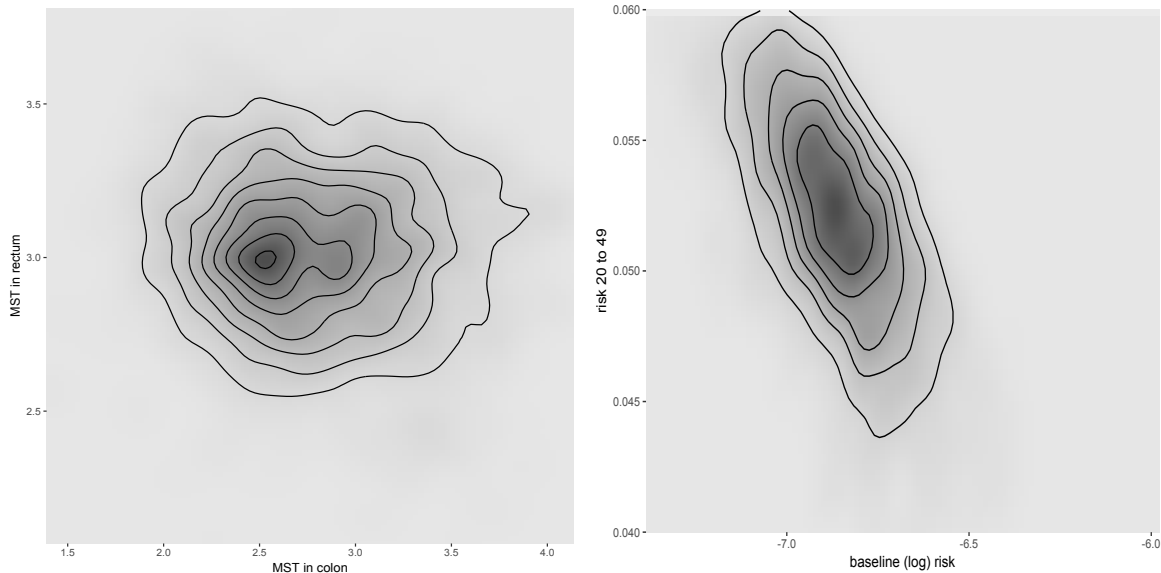


Figure 1: Left: Posterior distribution of mean sojourn time in the colon and the rectum. Right: Posterior distribution of the parameter α_{20} , which represents the annual increase in risk between the ages of 20 and 50 years, and baseline log adenoma risk.

sistent with calibration targets. Advantages of IMABC include clear stopping rules based on the a specified effective sample, the ability to specify which targets are most important through tolerance intervals, and the ability to take advantage of parallelized code. We illustrated the use of IMABC by calibrating a MSM for colorectal cancer, a real-world problem with a relatively high dimensional parameter space and multiple calibration targets.

The validity of ABC algorithms, in the sense that they result in samples from the approximate posterior distribution $f(\theta \mid \rho(y, y^*) < \epsilon)$, relies on the validity of the corresponding exact algorithms. IMABC is an approximate Bayesian version of adaptive importance sampling, similar to IMIS, with samples drawn from the parameter space using a proposal distribution that is a mixture of normal distributions. Posterior estimates are based on accepted draws that are weighted to account for differences between the prior and proposal distributions. In terms of ABC approaches, IMABC is most similar to the ABC-PMC approach (Beaumont et al., 2009). IMABC adds new points in the region near a subset of points that produce simulated targets closest to observed targets, whereas ABC-PMC samples points based on an approximation to the joint distribution using importance weights. The IMABC algorithm allows for locally adaptive covariance matrices that vary across components, and uses a new approach to selecting tolerance levels, based on α -levels associated with a test of equality between the simulated and observed targets, which implicitly incorporation of the precision of calibration targets.

A limitation of the IMABC algorithm as applied to MSM calibration is that it is computationally demanding. We implemented IMABC as a dynamic high-performance computing (HPC) workflow via the EMEWS framework (Ozik et al., 2016). Future work will explore the release of publicly available code to allow others to utilize these approaches in other computing environments. Because

calibration to summary statistics requires simulation of a large number of model evaluations, each with a large number of agents, we plan to explore ways to improve the efficiency of IMABC model calibration, such as guidance regarding user-selected tuning parameters. Finally, we plan to examine efficient approaches to parameter updating when new targets become available, and sequential calibration approaches that can be used to build from simple to more complex models.

Acknowledgements

This publication was made possible by financial support provided by NIH. Drs. Rutter and DeYoreo were supported by a grant from the National Cancer Institute (U01-CA-199335) as part of the Cancer Intervention and Surveillance Modeling Network (CISNET). Drs. Ozik and Collier were supported by the NIH (grants 1R01GM115839, 1S10OD018495), the NCI-DOE Joint Design of Advanced Computing Solutions for Cancer program, and through resources provided by the Computation Institute and the Biological Sciences Division of the University of Chicago, the University of Chicago Research Computing Center, and Argonne National Laboratory. This material is based upon work supported by the U.S. Department of Energy, Office of Science, under contract number DE-AC02-06CH11357. The contents of this article are solely the responsibility of the authors and do not necessarily represent the official views of the National Cancer Institute.

References

- Beaumont, M. A., Corneaut, J., Marin, J. M., and Robert, C. P. (2009), “Adaptive approximate Bayesian computation,” *Biometrika*, 96(4), 983–990.
- Blatt, L. J. (1961), “Polyps of the colon and rectum: Incidence and distribution,” *Diseases of the Colon and Rectum*, 4, 277–282.
- Blum, M., and Francois, O. (2010), “Non-linear regression models for Approximate Bayesian Computation,” *Statistics and Computing*, 20, 63–73.
- Bombi, J. A. (1988), “Polyps of the colon in Barcelona, Spain,” *Cancer*, 61, 1472–1476.
- Centers for Disease Control & Prevention (2011), “Vital signs: Colorectal cancer screening, incidence, and mortality—United States, 2002–2010,” *Morbidity and mortality weekly report*, 60(26), 884.
- Chapman, I. (1963), “Adenomatous polypi of large intestine: Incidence and distribution,” *Annals of Surgery*, 157, 223–226.
- Church, J. M. (2004), “Clinical Significance of Small Colorectal Polyps,” *Dis Colon Rectum*, 47, 481–485.

- Conlan, A. J. K., McKinley, T. J., Karolemeas, K., Pollock, E. B., Goodchild, A. V., Mitchell, A. P., Birch, C. P. D., Clifton-Hadley, R. S., and Wood, J. L. N. (2012), “Estimating the Hidden Burden of Bovine Tuberculosis in Great Britain,” *PLOS Computational Biology*, 8(10), 1–14.
URL: <https://doi.org/10.1371/journal.pcbi.1002730>
- Corley, D. A., Jensen, C. D., Marks, A. R., Zhao, W. K., De Boer, J., Levin, T. R., Doubeni, C., Fireman, B. H., and P, Q. C. (2013), “Variation of Adenoma Prevalence by Age, Sex, Race and colon Location in a Large Population: Implications for Screening and Quality Programs,” *Clinical Gastroenterology and Hepatology*, 11, 172–180.
- de Koning, H. J., Meza, R., Plevritis, S. K., Ten Haaf, K., Munshi, V. N., Jeon, J., Erdogan, S. A., Kong, C. Y., Han, S. S., van Rosmalen, J. et al. (2014), “Benefits and harms of computed tomography lung cancer screening strategies: a comparative modeling study for the US Preventive Services Task Force,” *Annals of internal medicine*, 160(5), 311–320.
- Eide, T. J., and Stalsberg, H. (1978), “Polyps of the large intestine in Northern Norway,” *Cancer*, 42, 2839–2848.
- Gille, U., and Salomon, F. V. (2000), “Brain growth in mallards, Pekin and Muscovy ducks (Anatidae),” *Journal of Zoology*, 252, 399–404.
- Hixson, L., Fennerty, M., Sampliner, R., McGee, D., and Garewal, H. (1990), “Prospective study of the frequency and size distribution of polyps missed by colonoscopy,” *J Natl Cancer Inst*, 82, 1769–1772.
- Imperiale, T. F., Wagner, D. R., Lin, C. Y., Larkin, G. N., Rogge, J. D., and Ransohoff, D. F. (2000), “Risk of Advanced Proximal Neoplasms in Asymptomatic Adults According to the Distal Colorectal Findings,” *NEJM*, 343, 169–174.
- Janoschek, A. (1957), “Das reaktionskinetische Grundgesetz und seine Beziehungen zum Wachstums- und Ertragsgesetz,” *Stat Vjschr*, 10, 25–37.
- Johannsen, L. G. K., Momsen, O., and Jacobsen, N. O. (1989), “Polyps of the large intestine in Aarhus, Demark. An autopsy study,” *Cancer*, 24, 799–806.
- Kim, J. J., Burger, E. A., Regan, C., and Sy, S. (2017), Screening for Cervical Cancer in Primary Care: A Decision Analysis for the U.S. Preventive Services Task Force., Technical report. Contract No. HHS-290-2012-00015-I.
- Kish, L. (1965), *Survey sampling*, New York, USA: John Wiley and Sons.
- Knudsen, A. B., Zauber, A. G., Rutter, C. M., Naber, S. K., Doria-Rose, V. P., Pabiniak, C., Johanson, C., Fischer, S. E., Lansdorp-Vogelaar, I., and Kuntz, K. M. (2016), “Estimation of benefits, burden, and harms of colorectal cancer screening strategies: modeling study for the US Preventive Services Task Force,” *Jama*, 315(23), 2595–2609.

- Kong, C. Y., McMahon, P. M., and Gazelle, G. S. (2009), “Calibration of Disease Simulation Model Using an Engineering Approach,” *Value in Health*, 12(4), 521–529.
URL: <http://dx.doi.org/10.1111/j.1524-4733.2008.00484.x>
- Leslie, A., Carey, F. A., Pratt, N. R., and Steele, R. J. C. (2002), “The colorectal adenoma–carcinoma sequence,” *British Journal of Surgery*, 89, 845–860.
- Lieberman, D. A., Weiss, D. G., Bond, J. H., Ahnen, D. J., Garewal, H., and Chejfec, G. (2000), “Use of Colonoscopy to Screen Asymptomatic Adults for Colorectal Cancer,” *NEJM*, 343, 162–168.
- Lieberman, D., Moravec, M., Holub, J., Michaels, L., and Eisen, G. (2008), “Polyp Size and Advanced Histology in Patients Undergoing Colonoscopy Screening: Implications for CT Colonography,” *Gastroenterology*, 135, 1100–1105.
- Liu, J. (2004), *Monte Carlo Strategies in Scientific Computing*, New York: Springer Verlag.
- Mandelblatt, J. S., Stout, N. K., Schechter, C. B., Van Den Broek, J. J., Miglioretti, D. L., Krapcho, M., Trentham-Dietz, A., Munoz, D., Lee, S. J., Berry, D. A. et al. (2016), “Collaborative modeling of the benefits and harms associated with different US breast cancer screening strategies,” *Annals of internal medicine*, 164(4), 215–225.
- Marin, J.-M., Pudlo, P., Robert, C. P., and Ryder, R. J. (2012), “Approximate Bayesian computational methods,” *Statistics and Computing*, 22(6), 1167–1180.
- Marjoram, P., Molitor, J., Plagnol, V., and Tavaré, S. (2003), “Markov chain Monte Carlo without likelihoods,” *Proceedings of the National Academy of Sciences*, 100(26), 15324–15328.
- McKinley, T., Vernon, I., Andrianakis, I., McCreesh, N., Oakley, J., Nsubuga, R., Goldstein, M., and White, R. (2017), “Approximate Bayesian Computation and simulation-based inference for complex stochastic epidemic models,” *Statistical science*, to appear.
- Meissner, H. I., Breen, N., Klabunde, C. N., and Vernon, S. W. (2006), “Patterns of colorectal cancer screening uptake among men and women in the United States,” *Cancer Epidemiology and Prevention Biomarkers*, 15(2), 389–394.
- Muto, T., Bussey, H. J. R., and Morson, B. C. (1975), “The Evolution of Cancer in the Colon and Rectum,” *Cancer*, 36, 2251–2270.
- National Cancer Institute (2004), “Surveillance, Epidemiology, and End Results (SEER) Program,”. released April 2004, based on the November 2003 submission.
URL: www.seer.cancer.gov
- National Center for Health Statistics (2000), “US Life Tables,”.
URL: <http://www.cdc.gov/nchs/products/pubs/pubd/lftbls/life/1966.htm>

- Nelder, J. A., and Mead, R. (1965), “A simplex method for function minimization,” *Computer Journal*, 7, 308–313.
- Ozik, J., Collier, N. T., Wozniak, J. M., and Spagnuolo, C. (2016), “From desktop to Large-Scale Model Exploration with Swift/T,” in *2016 Winter Simulation Conference (WSC)*, pp. 206–220.
- Pickhardt, P. J., Choi, R., Hwang, I., Butler, J. A., Puckett, M. L., Hildebrandt, H. A., Wong, R. K., Nugent, P. A., Mysliwiec, P. A., and Schindler, W. R. (2003), “Computed Tomographic Virtual Colonoscopy to Screen for Colorectal Neoplasia in Asymptomatic Adults,” *NEJM*, 349, 2191–2200.
- Ponugoti, P. L., and Rex, D. K. (2017), “Yield of a second screening colonoscopy 10 years after an initial negative examination in average-risk individuals,” *Gastrointestinal endoscopy*, 85(1), 221–224.
- Pritchard, J. K., Seielstad, M. T., Perez-Lezaun, A., and Feldman, M. W. (1999), “Population growth of human Y chromosomes: a study of Y chromosome microsatellites,” *Molecular Biology and Evolution*, 16(12), 1791–1798.
URL: + <http://dx.doi.org/10.1093/oxfordjournals.molbev.a026091>
- Raftery, A., and Bao, L. (2010), “Estimating and Projecting Trends in HIV/AIDS Generalized Epidemics Using Incremental Mixture Importance Sampling,” *Biometrics*, 66, 1162–1173.
- Ratmann, O., Camacho, A., Meijer, A., and Donker, G. (2014), “Statistical modelling of summary values leads to accurate approximate Bayesian computations,” *ArXiv*, arXiv:1305.4283.
- Rex, D., Cutler, C., Lemmel, G., Rahmani, E., Clark, D., Helper, D., Lehman, G., and Mark, D. (1997), “Colonoscopic miss rates of adenomas determined by back-to-back colonoscopies,” *Gastroenterology*, 112, 24–28.
- Rickert, R. R., Auerbach, O., Garfinkel, L., Hammond, E. C., and Frasca, J. M. (1979), “Adenomatous lesions of the large bowel. An autopsy survey,” *Cancer*, 43, 1847–1857.
- Rubin, D. (1987), “The calculation of posterior distributions by data augmentation: Comment: A noniterative sampling/importance resampling alternative to the data augmentation algorithm for creating a few imputations when fractions of missing information are modest: The SIR algorithm,” *Journal of the American Statistical Association*, 82, 543–546.
- Rutter, C. M., Johnson, E. A., Feuer, E. J., Knudsen, A. B., Kuntz, K. M., and Schrag, D. (2013), “Secular trends in colon and rectal cancer relative survival,” *Journal of the National Cancer Institute*, 105(23), 1806–1813.
- Rutter, C. M., Knudsen, A. B., Marsh, T. L., Doria-Rose, V. P., Johnson, E., Pabiniak, C., Kuntz, K. M., van Ballegooijen, M., Zauber, A. G., and Lansdorp-Vogelaar, I. (2016), “Validation of Models Used to Inform Colorectal Cancer Screening Guidelines: Accuracy and Implications,” *Medical Decision Making*, 36, 604–614.

- Rutter, C. M., Miglioretti, D. L., and Savarino, J. E. (2009), “Bayesian Calibration of Microsimulation Models,” *JASA*, 104, 1338–1350.
- Rutter, C. M., and Savarino, J. E. (2010), “An Evidence-Based Microsimulation Model for Colorectal Cancer: Validation and Application,” *Cancer Epidemiology Biomarkers and Prevention*, 19, 1992–2002.
- Sisson, S. A., Fan, Y., and Tanaka, M. M. (2007), “Sequential Monte Carlo without likelihoods,” *Proceedings of the National Academy of Sciences*, 104(6), 1760–1765.
URL: <http://www.pnas.org/content/104/6/1760.abstract>
- Steele, R., Raftery, A., and Edmond, M. (2006), “Computing Normalizing Constants for Finite Mixture Models via Incremental Mixture Importance Sampling (IMIS),” *Journal of Computational and Graphical Statistics*, 15, 712–734.
- Stemmermann, G. N., and Yatani, R. (1973), “Diverticulosis and polyps of the large intestine. A necropsy study of Hawaii Japanese,” *Cancer*, 31, 1260–1270.
- Szczepanski, W., Urban, A., and Wierzchowski, W. (1992), “Colorectal polyps in autopsy material. Part I. Adenomatous polyps,” *Pat Pol*, 43, 79–85.
- Tavare, S., Balding, D., Griffiths, R., and Donnelly, P. (1997), “Inferring Coalescence Times from DNA Sequence Data,” *Genetics*, 145, 505–518.
- Toni, T., Welch, D., Strelkowa, N., and Stumpf, M. (2009), “Approximate Bayesian computation scheme for parameter inference and model selection in dynamical systems,” *Journal of the Royal Society Interface*, 6(31), 187–202.
- Williams, A. R., Balasooriya, B. A. W., and Day, D. W. (1982), “Polyps and cancer of the large bowel: A necropsy study in Liverpool,” *Gut*, 23, 835–842.
- Winawer, S. J., Fletcher, R. H., Miller, L., Godlee, F., Stolar, M., Mulrow, C., Woolf, S., Glick, S., Ganiats, T., Bond, J. et al. (1997), “Colorectal cancer screening: clinical guidelines and rationale,” *Gastroenterology*, 112(2), 594–642.
- Wozniak, J. M., Armstrong, T. G., Wilde, M., Katz, D. S., Lusk, E., and Foster, I. T. (2013), “Swift/T: Large-Scale Application Composition via Distributed-Memory Dataflow Processing,” in *2013 13th IEEE/ACM International Symposium on Cluster, Cloud, and Grid Computing*, pp. 95–102.